EXHIBIT A

Langmuir 1993, *9*, 3050–3056

Adsorption and Coprecipitation of Single Heavy Metal Ions onto the Hydrated Oxides of Iron and Chromium

Russell J. Crawford,* Ian H. Harding, and David E. Mainwaring

Centre for Applied Colloid and BioColloid Science, Department of Applied Chemistry, Swinburne University of Technology, P.O. Box 218, Hawthorn 3122, Australia

Received January 11, 1993. In Final Form: July 15, 1993[a]

The adsorption and coprecipitation characteristics of Cr(III), Ni(II), and Zn(II) with amorphous iron(III) oxide and Ni(II) and Zn(II) with amorphous chromium(III) oxide have been measured and modeled using the James–Healy model for metal ion adsorption.[1] The results for the adsorption and the coprecipitation experiments have been compared. In all systems, coprecipitation is more efficient than adsorption although in the case of Zn(II) removal by amorphous iron(III) oxide the difference was minimal. The contributions of the chemical free energy of adsorption to the overall adsorption free energy changes have been determined and found to be greater for coprecipitation than for adsorption, greater for Zn(II) than for Ni(II), and greater for hydrated amorphous chromium(III) oxide than for hydrated amorphous iron(III) oxide.

Introduction

Precipitation, adsorption, and coprecipitation of heavy metals find an increasingly important role in many technological processes such as the formation of ceramic and metallic precursors. These phenomena are also currently being used to remove heavy metals from wastewater streams in adsorbing colloid flotation techniques.[2-5] In this process, metal ions are adsorbed onto the surfaces of colloids which are then removed from suspension by a concentration mechanism such as foam flotation. Coprecipitation and adsorption processes are also thought to be important controlling phenomena dictating the concentration of metal ions in the environment.[6]

The distinction between simple precipitation, coprecipitation, and adsorption is not always clear. Figure 1 illustrates these processes as defined in this study. It is well-known[7] that increasing the pH of a heavy metal ion will eventually result in the formation of an insoluble metal hydroxide precipitate. This simple mechanism for removal of metal ions is commonly used in waste treatment processes with no further sophistication required. Simple hydroxide precipitation typically results in a sharp sigmoidal removal profile. At very high pH levels redissolution of the metal hydroxide may occur; however this is not shown in Figure 1 since it is the initial removal which is of interest, and even when thermodynamically favoured, redissolution is often slow to occur. Adsorption processes can also occur whenever a solid substrate surface is present and also typically result in a similar sigmoidal isotherm, commonly not as steep as that observed for simple hydroxide precipitation. Preforming of the colloid involves pH adjustment which must be performed in the absence of the heavy metal ions to be removed from solution. pH adjustment of the heavy metal ions to be removed is then achieved simply by adding the pH adjusted preformed colloid. It is well-known[1,8-11] that adsorption processes occur at a lower pH than that of simple hydroxide precipitation, as indicated in Figure 1. In the case of adsorption, the solid substrate is preformed prior to [illegible] the metal ion to be removed from solution. Coprecipitation processes are subtly different to adsorption processes. In the case of coprecipitation the solid substrate is formed in the presence of the metal ion to be removed

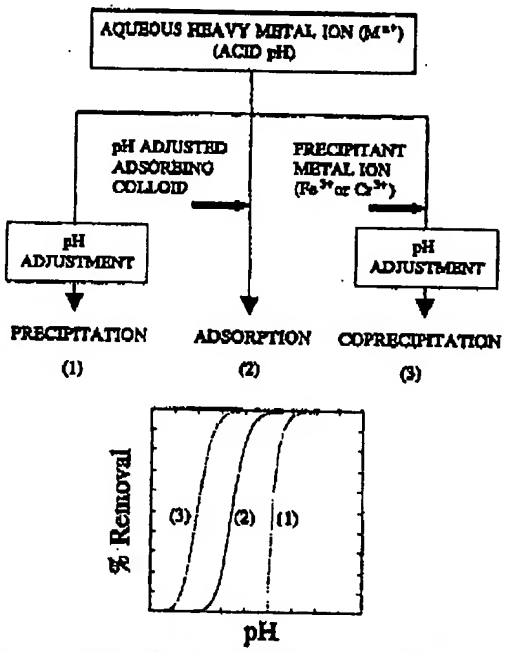

Figure 1. Schematic representation of the three processes responsible for the removal of heavy metal ions from solution.

[a] Abstract published in *Advance ACS Abstracts*, September 15, 1993.

(1) James, R. O.; Healy, T. W. *J. Colloid Interface Sci.* 1972, *40* (1) [illegible].
(2) Clarke, A. N.; Wilson, D. J. In *Foam Flotation: Theory and Applications*; Marcel Dekker: New York, 1983.
(3) Robertson, R. P.; Wilson, D. J.; Wilson, C. S. *Sep. Sci. Technol.* 1976, *11* (8), 669.
(4) De Carlo, E. H.; Zaitlin, H.; Fernando, Q. *Anal. Chem.* 1981, *53*, 1104.
(5) Sanciolo, P.; Harding, I. H.; Mainwaring, D. E. *Sep. Sci. Technol.* 1992, *27* (3), 376.
(6) James, E. A. In *Trace Elements Sorption by Sediments and Soils—Sites and Processes*; Chappel, W., Peterson, K., Eds.; Dekker: New York, 1977; Vol. 2.
(7) Day, R. A.; Underwood, A. L. *Quantitative Analysis*, 3rd ed.; Prentice-Hall: Englewood Cliffs, NJ, 1974; Chapter 7.
(8) Benjamin, M. M.; Leckie, J. O. *Environ. Sci. Technol.* 1981, *15*, 1050.
(9) Benjamin, M. M.; Leckie, J. O. *Environ. Sci. Technol.* 1982, *16*, 162.
(10) James, R. O.; Healy, T. W. *J. Colloid Interface Sci.* 1972, *40* (1), 42.
(11) James, R. O.; Healy, T. W. *J. Colloid Interface Sci.* 1972, *40* (1), 53.

0743-7463/93/2409-3050$04.00/0

from solution. While the enhancement of removal by adsorption or coprecipitation over simple precipitation is well documented, the relationship between coprecipitation and adsorption is not as clear. Although few studies directly compare all three processes, particularly using a well-defined model surface, it is our belief that coprecipitation will enhance (i.e., shift to lower pH) the removal profile to an even greater extent than that of direct adsorption. This further enhancement either could be due to a greater binding strength for a coprecipitate surface (having multiple surface site types) over a simple precipitate surface (having a single surface type) or may simply be due to an effective increase in surface area for adsorption as colloidal particles are formed.

This paper aims to contribute to the understanding of removal processes by the direct comparison of hydroxide precipitation to both adsorption and coprecipitation processes involving the hydrated amorphous oxides of iron(III) and chromium(III) as model surfaces.

The James–Healy Model. The adsorption of single metal ions onto colloidal surfaces has been extensively investigated elsewhere[5,8,12-14] and many models for this process have been postulated.[1,15-17] In general, these models follow one of two different approaches: either a chemical equilibria approach[15,18] where experimentally determined equilibrium constants are used to quantify the adsorption phenomena or a free energy approach[1,10,11] where the relationship between the equilibrium constant and its related free energy change is exploited. Models based on thermodynamic free energy predictions are inherently more complex than simple equilibria approaches since all contributions to the adsorption process must be identified and accounted for. Thermodynamic modeling of metal ion adsorption should be thought of as still in its infancy since a large portion of the overall free energy is assigned to a specific chemical interaction term with little current understanding of the nature of its contribution.

James and Healy[1,10,11] in 1972 first proposed a quantitative model for adsorption of hydrolyzable metal ions at an oxide–water interface using a free energy approach. This model was interpreted in terms of the competition between Coulombic, chemical, and solvation free energy changes contributing to the overall free energy change associated with the adsorption process. Solvation energy changes are considered an unfavorable barrier to adsorption onto simple oxides and are a function of surface charge, valence of the adsorbing ion, and the dielectric constant of the solid adsorbent. Specific chemical free energy changes are considered as favorable to adsorption. Coulombic (electrostatic) free energy changes can be either favorable or unfavorable, depending on the pH of the solution and the isoelectric point of the colloid substrate. The free energy change resulting from the adsorption of species "i", $\Delta G^\circ_{\text{adsorption},i}$, is expressed as

$$\Delta G^\circ_{\text{adsorption},i} = \Delta G^\circ_{\text{Coulombic},i} + \Delta G^\circ_{\text{solvation},i} + \Delta G^\circ_{\text{chemical},i} \quad (1)$$

The equilibrium constant, K_i, is related to the free energy of adsorption by the expression

$$K_i = \exp\left(\frac{-\Delta G^\circ_{\text{adsorption},i}}{RT}\right) \quad (2)$$

The adsorption is assumed to be Langmuirian in form, giving the fraction of surface sites covered by the species "i" (θ_i), as

$$\theta_i = \frac{K_i M_i}{1 + \sum_i K_i M_i} \quad (3)$$

where M_i is the bulk concentration of adsorbing species "i".

The constituent parts of the free energy of adsorption (i.e. $\Delta G^\circ_{\text{Coulombic},i}$, $\Delta G^\circ_{\text{solvation},i}$, and $\Delta G^\circ_{\text{chemical},i}$) are given by James and Healy[1,10,11] as follows:

$$\Delta G^\circ_{\text{Coulombic},i} = z_i F \Delta\psi_x \quad (4)$$

$$\Delta\psi_x = \frac{2RT}{zF} \ln\left(\frac{(e^{zF\psi_0/2RT} + 1) + (e^{zF\psi_0/2RT} - 1)e^{-\kappa x}}{(e^{zF\psi_0/2RT} + 1) - (e^{zF\psi_0/2RT} - 1)e^{-\kappa x}}\right) \quad (5)$$

where z_i is the sign and the valence of the adsorbing ion, $\psi_0 = (2.303RT/zF)(\text{pH}_{\text{pzc}} - \text{pH})$, pH_{pzc} is the pH at the point of zero charge, $\kappa = (0.328 \times 10^{10})I^{1/2}$, I is the ionic strength, $x = (r_{\text{ion}} + 2r_w)$, r_{ion} is the radius of the adsorbing metal ion, r_w is the radius of water, and z is the charge of the background electrolyte

$$\Delta G_{\text{solvation},i} = \left(\frac{z_i^2 e^2 N_A}{16\pi\epsilon_0}\right)\left(\frac{1}{r_{\text{ion}} + 2r_w} - \frac{r_{\text{ion}}}{2(r_{\text{ion}} + 2r_w)^2}\right)\left(\frac{1}{\epsilon_{\text{int}}} - \frac{1}{\epsilon_{\text{bulk}}}\right) + \left(\frac{z_i^2 e^2 N_A}{32\pi\epsilon_0}\right)\left(\frac{1}{r_{\text{ion}} + 2r_w}\right)\left(\frac{1}{\epsilon_{\text{solid}}} - \frac{1}{\epsilon_{\text{int}}}\right) \quad (6)$$

where ϵ_{bulk} is the dielectric constant of the bulk water, ϵ_{int} is the dielectric constant of the interfacial area, ϵ_0 is the dielectric constant of a vacuum, e is the charge of an electron, and N_A is Avogadro's number. The dielectric constant of the interfacial region is calculated by

$$\epsilon_{\text{int}} = \left(\frac{\epsilon_{\text{bulk}} - 6}{1 + (1.2 \times 10^{-17})\left(\frac{d\psi}{dx}\right)_{r_w}^2}\right) + 6 \quad (7)$$

and

$$\frac{d\psi}{dx} = -2\kappa \frac{RT}{zF} \sinh\left(\frac{zF\Delta\psi_{r_w}}{2RT}\right) \quad (8)$$

The chemical free energy change ($\Delta G^\circ_{\text{chemical},i}$) is not calculated from an analytic expression but simply selected to provide a reasonable agreement between theory and experiment. This is justified in that a single $\Delta G^\circ_{\text{chemical},i}$ is used for all pH values and metal hydrolysis species. In this way, the adsorption isotherms are simply shifted across the pH axis with the other contributions to $\Delta G^\circ_{\text{adsorption},i}$ required to accurately predict the shape of the curve. It is not justified in the sense that a complete model would determine the components of $\Delta G^\circ_{\text{chemical},i}$ prior to any experimentation.

Various $\Delta G^\circ_{\text{chemical},i}$ values for specific metal/oxide systems have been reported.[1,17,19] These values are obtained experimentally and many values may be obtained for a variety of metal ion types on different oxide surfaces.

(12) Harding, I. H.; Healy, T. W. *J. Colloid Interface Sci.* **1985**, *107* (2), 382.
(13) Harding, I. H.; Healy, T. W. *J. Colloid Interface Sci.* **1984**, *107* (2), 371.
(14) Benjamin, M. M. *Environ. Sci. Technol.* **1983**, *17*, 686.
(15) Davis, J. A.; James, R. O.; Leckie, J. O. *J. Colloid Interface Sci.* **1978**, *63*, 480.
(16) Stumm, W.; Kummert, R.; Sigg, L. *Croat. Chem. Acta* **1980**, *53*, 291.
(17) Fuerstenau, D. W.; Osseo-Asare, K. *J. Colloid Interface Sci.* **1987**, *118* (2), 524.
(18) Schindler, P. W.; Furst, B.; Dick, B.; Wolf, P. U. *J. Colloid Interface Sci.* **1976**, *55*, 469.
(19) James, R. O.; Stiglich, P. J.; Healy T. W. *Faraday Discuss. Chem. Soc.* **1975**, *59*, 142.

Table I. Solution Equilibria and Equilibrium Constants

metal	equilibria	constant
chromium	$Cr^{3+}(aq) + H_2O \rightleftharpoons Cr(OH)^{2+}(aq) + H^+(aq)$	$p^*K_1 = 3.94$
	$Cr(OH)^{2+}(aq) + H_2O \rightleftharpoons Cr(OH)_2^+(aq) + H^+(aq)$	$p^*K_2 = 6.00$
	$Cr(OH)_2^+(aq) + H_2O \rightleftharpoons Cr(OH)_3(aq) + H^+(aq)$	$p^*K_3 = 9.10$
	$Cr(OH)_3(aq) + H_2O \rightleftharpoons Cr(OH)_4^-(aq) + H^+(aq)$	$p^*K_4 = 11.00$
	$Cr(OH)_3(ppt) \rightleftharpoons Cr^{3+}(aq) + 3OH^-(aq)$	$p^*K_{so} = 30.6$
nickel	$Ni^{2+}(aq) + H_2O \rightleftharpoons Ni(OH)^+(aq) + H^+(aq)$	$p^*K_1 = 8.76$
	$Ni(OH)^+(aq) + H_2O \rightleftharpoons Ni(OH)_2(aq) + H^+(aq)$	$p^*K_2 = 9.71$
	$Ni(OH)_2(aq) + H_2O \rightleftharpoons Ni(OH)_3^-(aq) + H^+(aq)$	$p^*K_3 = 10.52$
	$Ni(OH)_3^-(aq) + H_2O \rightleftharpoons Ni(OH)_4^{2-}(aq) + H^+(aq)$	$p^*K_4 = 11.29$
	$Ni(OH)_2(ppt) \rightleftharpoons Ni^{2+}(aq) + 2OH^-(aq)$	$p^*K_{so} = 16.1$
zinc	$Zn^{2+}(aq) + H_2O \rightleftharpoons Zn(OH)^+(aq) + H^+(aq)$	$p^*K_1 = 9.25$
	$Zn(OH)^+(aq) + H_2O \rightleftharpoons Zn(OH)_2(aq) + H^+(aq)$	$p^*K_2 = 10.16$
	$Zn(OH)_2(aq) + H_2O \rightleftharpoons Zn(OH)_3^-(aq) + H^+(aq)$	$p^*K_3 = 10.96$
	$Zn(OH)_3^-(aq) + H_2O \rightleftharpoons Zn(OH)_4^{2-}(aq) + H^+(aq)$	$p^*K_4 = 11.70$
	$Zn(OH)_2(ppt) \rightleftharpoons Zn^{2+}(aq) + 2OH^-(aq)$	$p^*K_{so} = 16.5$

Solution Chemistry. Three metal species, Cr(III), Ni(II), and Zn(II) were adsorbed or coprecipitated using amorphous iron(III) or chromium(III) oxide colloid. These metal ions were selected for analysis because of their prevalence in industrial wastewater streams.[5] Each of these metal ions undergoes hydrolysis to varying extents, the products of which, along with their hydrolysis and solubility product constants, are given in Table I. The values used were the average of several literature values[20-22] with some small adjustments to give a self-consistent set of equilibria.

Experimental Section

1. Sample Preparation. All reagents used in the adsorption and coprecipitation trials were of AR quality unless otherwise specified. All solutions were prepared in 10^{-2} M KNO_3 background electrolyte solution. The electrolyte solution was prepared using high-purity water, which possessed a specific conductivity less than 1.0×10^{-6} Ω^{-1} cm^{-1} and a surface tension of 72.8 mN m^{-1} at 20 °C. The pH was measured using an Orion Research pH meter (Model 701A) which was calibrated using Merck Titrisol buffers at pH 4.00 and 9.00. The buffers were prepared using 10^{-2} M KNO_3 solution. All pH adjustments were made using potassium hydroxide solution.

pH adjustments and equilibration took place in a jacketed flange flask reaction vessel which was maintained at 25 °C. All pH adjustments, pH measurements, reagent additions, and sample removals were performed through ground glass connections in the top of the vessel. High-purity nitrogen (which was scrubbed using acid, base, and a silica suspension) was used to degas any solutions before pH adjustments were made, ensuring a CO_2-free atmosphere for equilibration.

The degree of metal ion removal during the various adsorption or coprecipitation experiments was evaluated by determining the concentration of the metal ion remaining in solution after equilibration had taken place. Samples were removed, filtered through a 0.22-μm Millipore nitrocellulose filter, acidified, and analyzed using a Varian SpectrAA-20 atomic absorption spectrometer.

All metal ion solutions were prepared from the nitrates. The adsorbing metal ions were of concentration 50 ppm (with respect to the metal ion) as this was the approximate concentration found in industrial effluent having significant metal ion contamination. The adsorbing or coprecipitated colloid was of concentration 250 ppm with respect to either Fe(III) or Cr(III). Metal ion adsorption trials using amorphous hydrous metal oxide substrates are generally described in terms of the concentration (ppm) of metal ion which has been used to form the colloidal adsorbent rather than its corresponding specific surface area (m^2 L^{-1}).[4,9] The reason for this lies in the pseudoequilibrium nature of the colloid(s) formed.[23] Traditional surface area measurement techniques for analysis of amorphous hydrous metal oxides give very different values depending on the treatment of the colloid (e.g. dilution, drying time, etc.) and the exact methodology. Metal ion adsorption, in fact, provides a more appropriate approach for the determination of the surface area available on such hydrous adsorbents in solution. In this study adsorption results have been used to obtain the surface area of the colloidal suspensions, which were 60 m^2 L^{-1} for amorphous iron(III) oxide and 53 m^2 L^{-1} for amorphous chromium(III) oxide. These surface areas were self-consistent for all of the metal adsorbates studied.

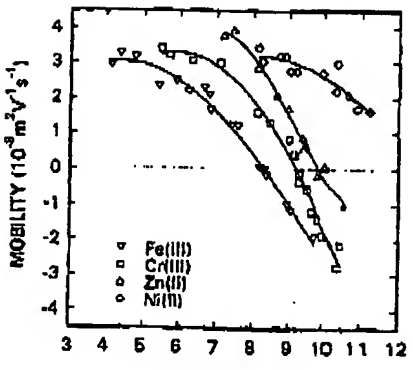

Figure 2. Electrophoretic mobility of amorphous iron(III), chromium(III), zinc(II), and nickel(II) oxides.

The isoelectric points of amorphous iron(III) and chromium(III) oxide were measured using a DELSA 440 (Coulter Electronics) by the normal method of measuring the electrophoretic mobility as a function of pH, as shown in Figure 2. The DELSA 440 instrument uses a Doppler light scattering effect to determine the electrophoretic mobility of the appropriate sample. In this study there was no requirement of dilute, or otherwise alter, the suspension concentration used during adsorption and coprecipitation experiments since the percent solids was below the threshold at which light scattering for this instrument (and for this particle size) becomes invalid. Included in Figure 2 are the electrophoretic mobility curves for amorphous zinc(II) and nickel(II) oxides for comparison. The isoelectric points found in this study were 8.2 for iron(III) oxide, 9.2 for chromium(III) oxide, 9.8 for zinc(II) oxide, and >12 for nickel(II) oxide. The values for iron(III) oxide and zinc(II) oxide are consistent with those given by Parks[24] of 8.0 and 9.3, respectively; however the value for amorphous chromium(III) oxide is considerably higher than that given by Parks[24] of 7.0. Interestingly, however, our value of 9.2 for amorphous chromium(III) oxide is consistent with Parks' general theory relating isoelectric point to the physical properties of the metal ion used to form the oxide.

2. Precipitation, Adsorption, and Coprecipitation Studies. The kinetics of adsorption have been discussed by various workers.[12,24-26] Heavy metal cations have been shown to undergo not only a fast initial adsorption step but also a slower adsorption step which can occur over periods of time ranging from days to several weeks.[25] The equilibration time selected in this study was 40 min, which allows only for the fast adsorption/coprecipitation step. Experiments were carried out in three modes: direct precipitation, adsorption, and coprecipitation.

Direct precipitation of single metal ions was obtained by slowly adjusting the pH of the metal nitrate solutions which were 50 ppm with respect to the metal ion in question. The pH and extent of precipitation were measured after equilibration at the final pH for 40 min. The experiment was repeated with a fresh sample for each pH measured.

(20) Sillén, L. G.; Martell, A. E. *Stability Constants*; Chem. Soc. (London), Special Publ. 17; Metcalfe and Cooper: London, 1971.
(21) Sillén, L. G.; Martell, A. E. *Stability Constants, Supplement No. 1*; Chem. Soc. (London), Special Publ. 25; Metcalfe and Cooper: London, 1971.
(22) James, R. O. Ph.D. Thesis, University of Melbourne, 1971.
(23) Parks, G. A. *Chem. Rev.* 1965, *65*, 177.
(24) Bunzyl, K.; Schmidt, W.; Sansoni, B. *J. Soil Sci.* 1976, *27*, 32.
(25) Zasoski, R. J.; Burau, R. G. *Soil Sci. Soc. Am. J.* 1978, *42*, 372.
(26) Gadde, R.; Laitinen, H. *Anal. Chem.* 1974, *46*, 2022.

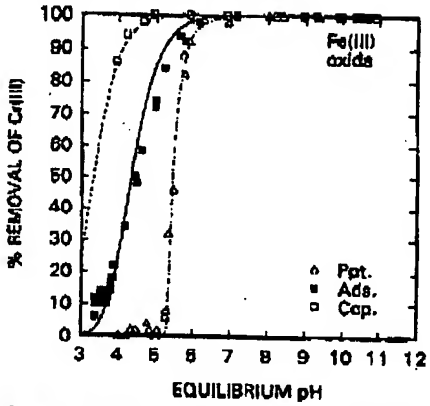

Figure 3. Adsorption and coprecipitation of Cr(III) (50 ppm) with amorphous iron(III) oxide (250 ppm) compared to precipitation of Cr(III) (50 ppm) alone. $\Delta G°_{chemical}$: adsorption, −50 kJ mol^{-1}; coprecipitation, −61 kJ mol^{-1}.

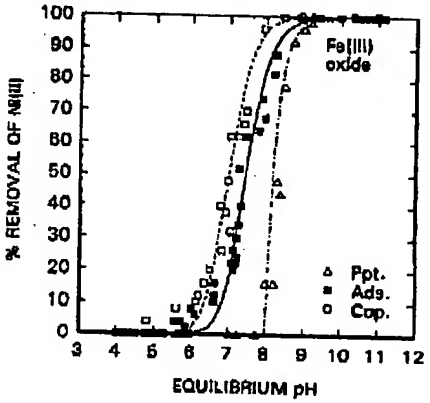

Figure 4. Adsorption and coprecipitation of Ni(II) (50 ppm) with amorphous iron(III) oxide (250 ppm) compared to precipitation of Ni(II) (50 ppm) alone. $\Delta G°_{chemical}$: adsorption, −33 kJ mol^{-1}; coprecipitation, −38 kJ mol^{-1}.

In the adsorption experiments, the adsorbing colloid (either amorphous iron(III) or chromium(III) oxide) was prepared by slowly increasing the pH of a 250 ppm iron(III) or chromium(III) nitrate solution. The adsorbing ion (Cr(III), Ni(II), or Zn(II)) was then added and equilibration allowed to take place, after which time the equilibrium pH of the suspension and extent of adsorption were measured. Again the experiment was repeated with a fresh sample for each pH measured.

In the coprecipitation experiments, the pH was slowly increased with the iron(III) or chromium(III) nitrate solution and the metal ion under investigation both present. Again, the pH and extent of coprecipitation were measured after equilibration in sample experiments at a single pH.

Results

1. Precipitation, Adsorption, and Coprecipitation [illegible] characteristics (precipitation, adsorption, and coprecipitation) using amorphous iron(III) oxide as the adsorbing or coprecipitated colloid are given in Figures 3–5 for Cr(III), Ni(II), and Zn(II), respectively. All three figures show the experimentally determined points and lines which show the isotherms of best fit obtained using the James–Healy model. The validity and details of the model curves will be discussed shortly. The $\Delta G°_{chemical}$ values required for optimal fit of the model to the data are listed with each figure.

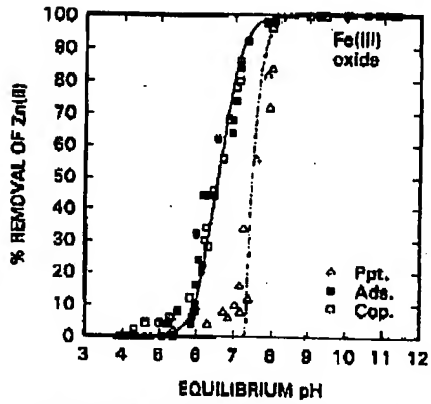

Figure 5. Adsorption and coprecipitation of Zn(II) (50 ppm) with amorphous iron(III) oxide (250 ppm) compared to precipitation of Zn(II) (50 ppm) alone. $\Delta G°_{chemical}$: adsorption, −45 kJ mol^{-1}; coprecipitation, −45 kJ mol^{-1}.

The concentration of Cr(III) in the aqueous phase changes from the initial added Cr(III) concentration (i.e., 0% removal) to nearly zero (i.e. 100% removal) over a narrow pH range. This pattern is characteristic for aqueous metal removal by adsorption or precipitation mechanisms (e.g., refs 1, 10, 12, 13, and 17). James and Healy,[1] for example, have shown that the adsorption of Cr(III) onto SiO_2 changes from approximately zero at pH 3.5 to 50% at pH 4.5 and 100% at pH 6.1. The pH range for adsorption of Cr(III) onto amorphous iron(III) oxide, given in Figure 3, is very similar.

The concentration of Ni(II) in the aqueous phase also changes from the initial added Ni(II) concentration to zero over a narrow pH range. The pH range over which Ni(II) is removed by adsorption in this study is 6.8–8.2 which is similar to that found by Osseo-Asare and Fuerstenau[17] for Ni(II) adsorption onto haematite, but dissimilar to that obtained by Kinniburgh et al.[27] for Ni(II) adsorption onto amorphous iron(III) oxide gel.

Zn(II) removal follows the same qualitative pattern as seen for Ni(II) and Cr(III). The adsorption curve shows an increase in adsorption ranging from zero at pH 6.0 to nearly 100% at pH 7.2. This pH range is consistent with the results of Benjamin[14] and Benjamin and Leckie;[28] however as was observed with Ni(II), these results are not consistent with Kinniburgh et al.[27] The pH range over which adsorption took place for Zn(II) onto amorphous iron(III) oxide gel was found by Kinniburgh et al. to be approximately 1 pH unit lower than the results presented here. Their Ni(II) data were also approximately 1 pH unit lower.

For each of the three metal ion adsorbates, the percentage removal of the metal ion in question is enhanced by the presence of an adsorbing surface at any given pH. The pH range over which adsorption (for example) takes place will depend to some extent on factors such as surface area and metal ion concentration; however the choice of [illegible] factor.[10] The extent of removal, at any given pH, resulting from coprecipitation is greater than the extent of removal resulting from adsorption for Cr(III) and less so for Ni(II) and the difference is barely perceptible for Zn(II).

2. Precipitation, Adsorption, and Coprecipitation with Amorphous Chromium(III) Oxide. Similar re-

(27) Kinniburgh, D. G.; Jackson, M. L.; Syers, J. K. *Soil Sci. Soc. Am. J.* **1976**, *40*, 796.
(28) Benjamin, M. M.; Leckie, J. O. *J. Colloid Interface Sci.* **1981**, *79* (1), 209.

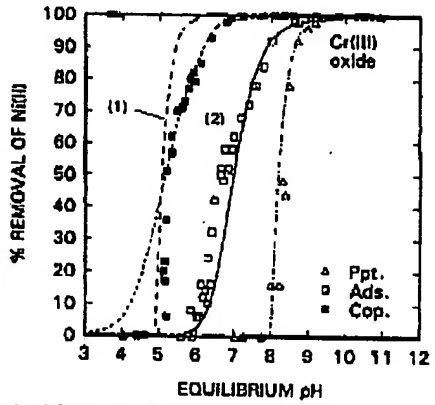

Figure 6. Adsorption and coprecipitation of Ni(II) (50 ppm) with amorphous chromium(III) oxide (250 ppm) compared to precipitation of Ni(II) (50 ppm) alone. $\Delta G^\circ_{chemical}$, adsorption, −44 kJ mol^{-1}; (1) precipitation isotherm for 250 ppm Cr(III); (2) coprecipitation, −64 kJ mol^{-1}.

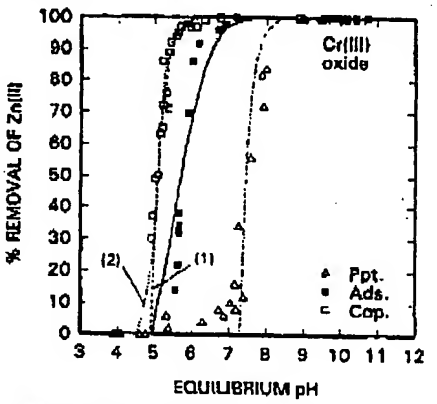

Figure 7. Adsorption and coprecipitation of Zn(II) (50 ppm) with amorphous chromium(III) oxide (250 ppm) compared to precipitation of Zn(II) (50 ppm) alone. $\Delta G^\circ_{chemical}$, adsorption, −62 kJ mol^{-1}; (1) precipitation isotherm for 250 ppm Cr(III); (2) coprecipitation, −75 kJ mol^{-1}.

moval experiments were performed using Ni(II) and Zn(II) with amorphous chromium(III) oxide as the adsorbing or coprecipitating colloid. It is not possible to perform a simple adsorption study of Fe(III) onto amorphous chromium(III) oxide since the iron(III) oxide forms at a lower pH than the chromium(III) oxide. Zn(II) adsorption onto amorphous chromium(III) oxide also proves difficult since complete precipitation of the chromium(III) oxide adsorbent surface is not achieved until after Zn(II) removal from solution has commenced. When the adsorption results are modeled, the total available surface area at a given pH was calculated as a fraction of the total possible surface area using Cr(III) precipitation data. For Ni(II) adsorption, however, the Cr(III) adsorbate surface is almost [illegible] and hence no adjustment of surface area is required.

The removal characteristics (precipitation, adsorption, and coprecipitation) using amorphous chromium(III) oxide as the adsorbing or coprecipitated colloid are given in Figures 6 and 7 for Ni(II) and Zn(II), respectively. Both figures show the experimentally determined points and lines which represent the isotherms of best fit obtained using the James–Healy model. The $\Delta G^\circ_{chemical}$ values required to obtain an optimal fit of the model to the data are listed with each figure. The coprecipitation curves in both cases lie close to the precipitation curve for Cr(III) obtained in the absence of the other metals and may simply reflect a physical entrainment as the removal mechanism. The precipitation curve for 250 ppm Cr(III) is included in Figures 6 and 7 for comparison with the coprecipitation curves.

Comparison of amorphous chromium(III) oxide with amorphous iron(III) oxide as the solid can be achieved by comparing Figure 4 with Figure 6, and by comparing Figure 5 with Figure 7. Amorphous iron(III) oxide is often chosen as an adsorbing substrate not simply because of the ease with which it can be obtained but also because of its recognized efficiency as an adsorbent.[6] The above comparison shows that amorphous chromium(III) oxide is an even more efficient adsorbing substrate (for a similar surface area).

Discussion

1. The James–Healy Model. A computer program of the model, incorporating the appropriate theoretically based equations, was used in this study. In addition to the solution equilibria referred to in the Introduction, this model requires specification of certain physical constants characteristic of the type of colloid used as a substrate. After extensive evaluation of the model parameters, it was found that the dielectric constant of the solid substrate plays a major role in determining the pattern of metal ion removal. For example, when using a solid substrate with a dielectric constant (ϵ) approaching that of water (ϵ = 78.3), such as titanium dioxide,[1] the model specifies the dominant adsorbing species to be the free metal ion (e.g., Zn^{2+}). The consequence of this is that the adsorption curve for titanium dioxide as a substrate is dominated by the change in $\Delta G^\circ_{Coulombic}$, which occurs as the pH changes. By contrast, when using a solid substrate with a low dielectric constant, for example silicon dioxide (ϵ = 6), the model specifies the dominant adsorbing species to be a hydrolysis product of the metal ion (i.e., $Zn(OH)^+$). The consequence of this is that an adsorption isotherm for a metal adsorbing onto a silicon dioxide substrate is dominated by the change in speciation of the adsorbing metal ion which occurs as the pH changes.

James and Healy,[1] among others, have shown that the hydrolysis of metal ions is directly correlated to their adsorption behavior when adsorbed onto a low dielectric constant solid. The dielectric constants used in this study were 14.2 for iron(III) oxide[29] and 8.0 for chromium(III) oxide.[30] By use of these values, the dominant adsorbing species in all systems studied here were found to be the first and/or second hydrolysis product(s). The model predicts that the free metal ion (Cr^{3+}, Ni^{2+}, or Zn^{2+}) has no significant or direct role in adsorption or coprecipitation using either amorphous iron(III) or chromium(III) oxides.

Systematic variation of the model parameters, such as dielectric constant, surface area, isoelectric point, and $\Delta G^\circ_{chemical}$, showed that all parameters except surface area were important in determining the exact species responsible for removal. Since it is very difficult to determine the actual dielectric constant relating to the colloidal phase of an amorphous oxide slurry, the use of literature values for the oxides may be considered a weakness in this approach; however an increase in the "true" dielectric constant would simply result in a lowering of the computed $\Delta G^\circ_{chemical}$ and this results in the same predicted isotherm.

(29) Dempsey, B. A.; Singer, P. C. *Contam. Sediments* **1980**, *2*, 333.
(30) Lal, H. B.; Srivastava, R.; Srivastava, K. G. *Phys. Rev.* **1967**, *154* (2), 505.

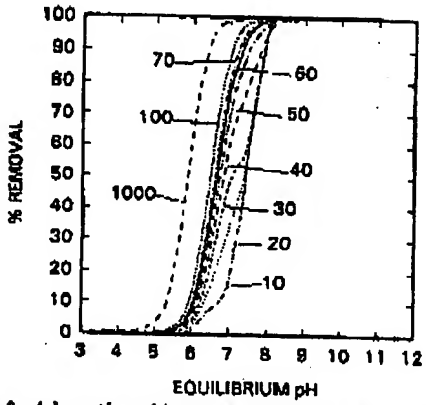

Figure 8. Adsorption of Zn(II) (50 ppm) onto amorphous iron-(III) oxide (250 ppm) as a function of specific surface area (in m^2 L^{-1}) as calculated using the James–Healy model. ($\Delta G^\circ_{chemical,i}$ = −45 kJ mol^{-1}).

Changing the isoelectric point has a strong influence over the overall position of the predicted removal isotherm. It should be noted that the James–Healy model does not account for the change in surface charge and, hence, potential brought about as a result of the adsorption or coprecipitation itself. At low removal, this will be a minor deficiency; however at higher removals it could introduce a large error. At these higher removals the electrostatic properties of the surface (and for that matter, the dielectric properties) will be influenced by, and move toward, that of the adsorbing metal oxide. The influence of the adsorbing ion on the solvation and electrostatic components of the model will be addressed in future work.

A parameter having surprisingly little influence over the predicted adsorbing species and the isotherm itself is surface area. The surface area of an amorphous substrate which is precipitated *in situ* is very difficult to obtain; however we have found that the model itself can be used to obtain a good approximation of the surface area to be used for modeling purposes. An example of the predicted adsorption removal dependence on surface areas is given in Figure 8 for Zn(II) adsorption with amorphous iron-(III) oxide. It can be seen in the curves obtained from the model that a "saturation" of the surface available for adsorption is reached at low surface areas. Subsequently, the curve follows the precipitation isotherm for the metal ion alone. At higher surface areas there is little change to the slope or shape of the curve allowing values between, for example, 60 and 100 m^2 L^{-1} to have little influence on the modeled curve. The surface area which is consistent with the adsorption data for all of the metal ion species involved in this study corresponds to a surface area of approximately 60 m^2 L^{-1} for the 250 ppm amorphous iron-(III) oxide. The surface area for the 250 ppm chromium-(III) oxide colloid, obtained by the same procedure, corresponds to approximately 53 m^2 L^{-1}. It is assumed in the modeling, that the surface area available for coprecipitation is the same as that available during adsorption experiments. Although this may cause a deviation of the modeled parameters (specifically $\Delta G^\circ_{chemical,i}$) from their true values, such a deviation should result in only a very small change in $\Delta G^\circ_{chemical,i}$ (see next section). Only if the change in surface area is substantial (more than 1 order of magnitude) would the $\Delta G^\circ_{chemical,i}$ required to model the data result in a significantly different descriptions of the coprecipitation process. It is unlikely that the surface area of coprecipitates would vary by an order of magnitude from the simple precipitates since the formation conditions and the resultant particle sizes were not seen to significantly alter. The latter point was confirmed since particle size information is a requirement for light scattering electrophoresis.

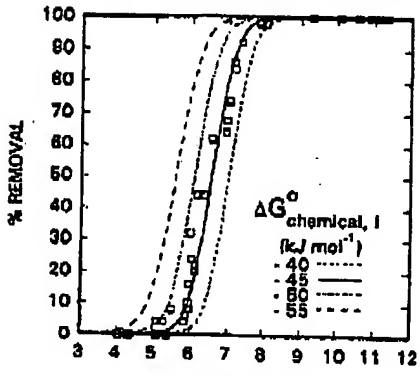

Figure 9. Adsorption of Zn(II) (50 ppm) with amorphous iron-(III) hydroxide (250 ppm) as a function of $\Delta G^\circ_{chemical,i}$ as calculated using the James–Healy model.

Table II. Chemical Free Energy Components of Adsorption and Coprecipitation

		$\Delta G^\circ_{chemical,i}$ (kJ mol^{-1})	
metal ion	colloid type	adsorption	coprecipitation
Cr(III)	iron(III) oxide	−50	−61
Ni(II)	iron(III) oxide	−33	−38
	chromium(III) oxide	−44	−64
Zn(II)	iron(III) oxide	−45	−45
	chromium(III) oxide	−62	−75

2. Comparison of $\Delta G^\circ_{chemical,i}$ Values. The chemical free energy contributions to the overall adsorption free energy were determined by fitting the theoretical isotherms to the experimental data. Examples of the isotherms dependence on $\Delta G^\circ_{chemical,i}$ are shown in Figure 9 for the case of Zn(II) adsorption onto an amorphous iron(III) oxide colloid surface. It is apparent from this figure that $\Delta G^\circ_{chemical,i}$ plays a major role in determining the position of the isotherm along the pH axis. As earlier mentioned, surface area also plays a role in determining the position of the isotherm along the pH axis; however comparison of Figures 8 and 9 shows that the $\Delta G^\circ_{chemical,i}$ is more influential. Even large errors in the estimation of surface area will be compensated in the modeling process by a slight error in $\Delta G^\circ_{chemical,i}$. Extensive testing has shown that relatively large changes in $\Delta G^\circ_{chemical,i}$ are required before any of the qualitative trends to be discussed shortly are affected.

The values for the chemical free energy contribution to the adsorption free energy for the three metals and two colloid types investigated may be compared in a single table. In this way the intrinsic strength of the binding between the metal ion and the substrate can be compared with the Coulombic (electrostatic) and coordination contributions factored out. The values obtained are summarized Table II.

It is difficult to directly compare these $\Delta G^\circ_{chemical,i}$ values with literature values since there are few such values available and importantly because adsorption may depend on experimental conditions such as the aging history[37] of the colloid used. Osseo-Asare and Fuerstenau[17] used several different $\Delta G^\circ_{chemical,i}$ values depending on the species "i". Their values for Ni(II) adsorption onto haematite were −21.7 kJ mol^{-1} for Ni^{2+} and $Ni(OH)^+$ and

−41 kJ mol^{-1} for higher hydrolysis species. Our value of −33 kJ mol^{-1} probably reflects an average of these values and results in a similar predicted adsorption isotherm.

A literature value obtained by James and Healy[1] also exists for Cr(III) adsorption onto SiO_2. The value (−29.3 kJ mol^{-1}) is considerably lower than that obtained in this study (−60 kJ mol^{-1}); however such a difference may not be surprising given the different substrates used.

3. Adsorption versus Coprecipitation. The results given in Figure 3–5 show that Cr(III), Ni(II), and Zn(II) removal from solution is enhanced by the presence of an amorphous iron(III) oxide colloid surface. Cr(III) in particular, and Ni(II) to a lesser extent, are even more efficiently removed by a coprecipitation mechanism rather than by adsorption onto the preformed colloid. The removal of Zn(II) from solution using the same colloidal system appears to be equally as efficient using either coprecipitation or adsorption. For both adsorption and coprecipitation the removal of metal ions (at a given pH) is considerably enhanced over their simple precipitation in the absence of a second colloidal surface.

Corey[31] has argued that the main difference between adsorption and coprecipitation lies in the geometry of the adsorbate surface; coprecipitation should be considered a three-dimensional process leading to a greater effective removal capacity than simple adsorption. Such an argument would predict considerably increased removal, at any given pH, for coprecipitation over adsorption. Surface area analysis as indicated in Figure 8, however, shows that the increase in effective surface area would need to be at least an order of magnitude larger to account for such an increased removal profile. Sion et al.[32] and Taylor[33] among others have presented evidence for the formation of mixed hydroxides of well-defined stoichiometry and solution behavior which differs from that of either hydroxide alone. One may thus speculate that the existence of such mixed hydroxide species during coprecipitation leads to enhanced removal over adsorption.

The results shown in Figures 6 and 7 show that Ni(II) and Zn(II) removal from solution is enhanced by the presence of an amorphous chromium(III) oxide colloid surface. Both adsorption and coprecipitation of Ni(II) or Zn(II) onto an amorphous chromium(III) oxide removes the metal ions to a greater extent than with the iron(III) oxide system. Again, the coprecipitation removal for either ion is greater than that achieved by adsorption alone, which is greater than direct precipitation alone.

Coprecipitation of Zn(II) with amorphous chromium(III) oxide removes Zn(II) according to the precipitation profile of Cr(III). Coprecipitation of Ni(II) with amorphous chromium(III) oxide appears to initially remove the Ni(II) according to the direct precipitation profile of the Cr(III) alone but is followed by a removal profile similar to adsorption once the Cr(III) has *completely* precipitated.

Comparisons of the removals shown in Figures 4 and 5 with the removals shown in Figures 6 and 7 show that amorphous chromium(III) oxide has a stronger adsorbing/coprecipitating binding strength than does amorphous iron(III) oxide. This is in contrast to the work performed by Harding and Healy[34] who have shown that there is little difference between a large number of adsorbing colloids, providing that their dielectric constants are all low. Harding and Healy[34] have argued, however, that some surfaces (such as latex) have an unusually high binding strength which is reflected by a large negative $\Delta G^\circ_{\text{chemical},i}$. Our results show that amorphous chromium(III) oxide also has a particularly large negative $\Delta G^\circ_{\text{chemical},i}$. They also show that Cr(III) as an adsorbate has a larger $\Delta G^\circ_{\text{chemical},i}$ than either Ni(II) or Zn(II). This unusual behavior when Cr(III) is present is difficult to rationalize, although it is noteworthy that Cr(III) also has an unusual solution chemistry in that its ligand exchange rate is very slow.[35] This could well result in structure at the adsorbing surface which is capable of enhancing adsorption by, for example, preventing adsorbed ions from readily desorbing and thus effectively shifting the equilibria to favor greater adsorption.

The ability of amorphous chromium(III) oxide to remove Ni(II) and Zn(II) more efficiently (at any given pH) than amorphous iron(III) oxide has considerable implications to the application of adsorption phenomena in the presence of Cr(III). Sanciolo et al.,[5] for example, have shown that metal ion removal using adsorbing colloid flotation is less efficient in waste effluent samples containing low Cr(III) concentrations. Our results show that this is presumably due to the enhancement of adsorption and coprecipitation by the formation of amorphous chromium(III) oxide. Further work will pursue whether or not the percentage removals obtained here can be enhanced even further by, for example, the presence of aqueous Cr(III) in the adsorption and coprecipitation of Ni(II) or Zn(II) using amorphous iron(III) oxide.

Conclusion

The adsorption and coprecipitation isotherms for Cr(III), Ni(II) and Zn(II) with amorphous iron(III) and chromium(III) oxides can be modeled using the James-Healy model for metal ion adsorption. Corresponding $\Delta G^\circ_{\text{chemical},i}$ values can be obtained from application of this model and show that there is an intrinsic difference in the adsorption thermodynamics between chromium(III) and iron(III) oxides.

The adsorption and coprecipitation isotherms for Zn(II) removal using amorphous iron(III) oxide are equivalent. There is a small but significant difference between adsorption and coprecipitation for Ni(II) and a large difference for Cr(III).

In all cases, coprecipitation was as efficient or more efficient than adsorption which was in turn more efficient than precipitation alone. Cr(III) was removed at a lower pH than Zn(II) which was removed at a lower pH than Ni(II) and amorphous chromium(III) oxide was a more efficient adsorbent than amorphous iron(III) oxide.

Acknowledgment. The authors thank Professor Tom Healy from the University of Melbourne for fruitful discussions regarding this research work.

(31) Corey, R. B. *Adsorption of Inorganics at Solid-Liquid Interfaces*; Anderson, M. A., Rubin, A. J., Eds.; Ann Arbor Science: Ann Arbor, MI, 1981.

(32) Sion, J.; Schultzl, W.; Volts, M. *Z. Anal. Chem.* 1971, *257*, 109.

(33) Taylor, H. F. W. *Min. Mag.* 1978, *39*, 377.

(34) Harding, I. H.; Healy, T. W. *Progs. Water Technol.* 1979, *11* (4/5), 265.

(35) Benson, D. *Mechanisms of Inorganic Reactions in Solution*; McGraw-Hill: London, 1968.